

## Scaling properties of wave functions and transport coefficients in quasicrystals

Takeo Fujiwara, Takashi Mitsui, and Susumu Yamamoto

*Department of Applied Physics, University of Tokyo, Bunkyo-ku, Tokyo 113, Japan*

(Received 4 December 1995)

Electronic wave functions and transport properties are presented in realistic crystalline approximants of decagonal Al-Cu-Co alloy, up to 4414 atoms in a unit cell. The system-size dependence of the participation ratio of wave functions shows that the wave functions of eigenstates show a power-law decay on average. The finite-size scaling analysis indicates that the diffusion constant decreases slowly with increasing system size, as a power of the system size. The scaling properties of the diffusion constant are discussed in connection with the spikiness of the density of states.

The electronic transport property in quasicrystals is quite exotic. The resistivity reaches several  $\Omega$  cm at very low temperatures<sup>1</sup> and the conductivity increases almost linearly with temperature.<sup>2</sup> Furthermore, the resistivity is enhanced in structurally ordered icosahedral quasicrystals.<sup>3</sup> The Drude peak cannot be observed in optical spectra of icosahedral quasicrystals.<sup>4</sup> The electronic transport<sup>5</sup> and optical properties<sup>6</sup> in decagonal quasicrystals are highly anisotropic. The resistivity parallel to the quasiperiodic plane is much higher than that along the periodic direction. The temperature dependence of the conductivity parallel to the quasiperiodic plane is similarly anomalous to that in icosahedral quasicrystals; on the other hand, that along the periodic direction is normal metallic.

Electronic structures and properties in realistic quasicrystals have been discussed theoretically by the present authors<sup>7</sup> and also by other groups.<sup>8</sup> The calculated electronic density of states (DOS) in crystalline approximants shows a deep depression, called the pseudogap, of width 0.5–1 eV at the Fermi energy,<sup>7,9–11</sup> and the pseudogap is observed experimentally in several quasicrystals and crystalline approximants.<sup>12</sup> The structural ordering dependence of the conductivity was explained in terms of the increasing number of transport channels with disorder.<sup>13</sup> The temperature dependence of the conductivity was also qualitatively explained by the existence of a set of sharp spikes with an individual width of 0.01 eV or even less ( $\approx 100$  K) in the DOS.<sup>7</sup>

Attempts to explain the anomalously low conductivity were made using the very flat energy dispersion (i.e., large effective masses) and the small number of energy bands crossing the Fermi energy (i.e., small carrier density), on the basis of calculated band structures, the Boltzmann formula, and realistic phenomenological values of the scattering time  $\tau$  (e.g.,  $10^{-14}$  s).<sup>7,10,11</sup> Of course, this cannot be a unique explanation because electron scattering is intrinsically due to the quasiperiodic structures and very much relates to the energy spectrum and wave functions.

The anomalous transport properties have sometimes been explained by weak localization theory.<sup>14</sup> A random system can be specified by the density of impurities, then the characteristic length scale is the average distance between impurities. On the other hand, in quasiperiodic systems, there is no characteristic length scale except interatomic (or inter-

cluster) distances and this fact is one of the reasons why we expect the power-law dependence of wave functions and conductance.<sup>15</sup> We believe the quantum interference effect at very low temperatures is important for its temperature and magnetic-field dependence. However, the anomalously large values and randomness dependence of the resistivity cannot be attributed to the quantum interference effect in weak localization theory. These phenomena are generic in quasiperiodic systems but not in random systems.

In this paper, we present the characteristics of the eigenstates of realistic crystalline approximants with up to 4414 atoms in a unit cell. The model structures of atomic arrangement were prepared by a three-step procedure. First, two-dimensional periodic Penrose tilings are constructed in a standard manner<sup>13,15</sup> and second, these are mapped to the binary alloy model, i.e., with two types of disks.<sup>16</sup> The third step is as follows: the large and small disks in the binary alloy model are mapped to large and small atomic clusters of transition metals (Co and Cu) and Al atoms with the help of the Burkov model,<sup>17</sup> which is constructed so as to be consistent with real-space imagery observed by electron microscope.<sup>18</sup> Atomic positions of Cu and Co in clusters were distinct from each other and identified by a stability consideration of the total electronic energy.<sup>11</sup> The two-dimensional layers are then stacked along the perpendicular  $c$  axis periodically.

The crystalline approximants used in the present work are approximately  $\text{Al}_{60}\text{Cu}_{28}\text{Co}_{12}$  and the total numbers of atoms are, respectively, 110, 644, 1686, 2728, and 4414 in a unit cell. These lattice units contain [1 wide ( $w$ ) and 0 narrow ( $n$ )], (4  $w$  and 3  $n$ ), (11  $w$  and 7  $n$ ), (18  $w$  and 11  $n$ ), and (29  $w$  and 18  $n$ ) rhombi, respectively. A wide rhombus consists of two large clusters (42 atoms each) and two small clusters (13 atoms each), and a narrow rhombus consists of one large and two small clusters.

The electronic structure were calculated by the tight-binding linear muffin-tin orbital (TB-LMTO) method, including  $s$ ,  $p$ , and  $d$  orbitals for each atom.<sup>19</sup> The potential parameters in the TB-LMTO method were determined self-consistently in the crystalline approximant of one wide tile of 110 atoms.<sup>11</sup> The periodic boundary condition is imposed on the two-dimensional quasiperiodic plane. The one-dimensional Bloch representation along the periodic  $c$ -direction are adopted for wave functions.

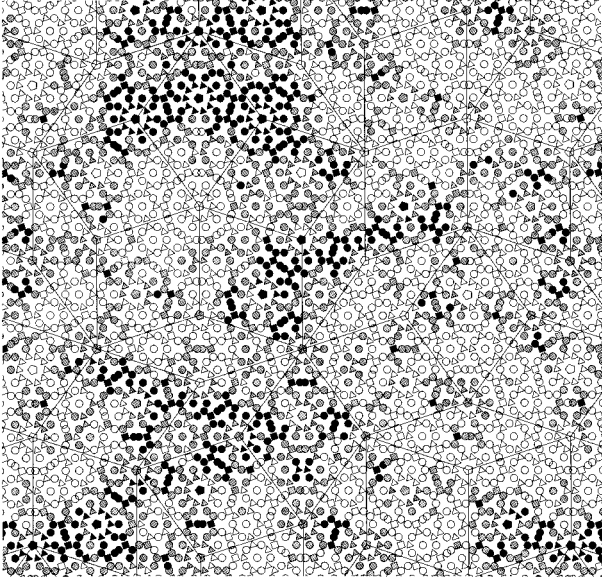


FIG. 1. A typical example of eigenstates near the Fermi energy ( $E = -0.041\ 32$  Ry) in a system of 2728 atoms in a unit cell. The symbols show atomic positions;  $\circ$ : Al,  $\triangle$ : Cu,  $\square$ : Co, which are on two layers. Those atoms represented by the solid symbols are most probable, with the total probability being 60%. Together, the shaded and closed symbols represent those atoms that have a total probability of 90%. The remaining atoms are represented by the open symbols.

The DOS in a larger crystalline approximant was calculated by the recursion method.<sup>20</sup> It must be noted that the recursion method cannot reproduce very fine structures of the DOS. The depth and width of the pseudogap ( $\sim 0.5$  eV wide) averaged over spikes are not affected seriously by the system size.

Exact eigenstates of a TB-LMTO Hamiltonian matrix with a fixed one-dimensional wavevector along the  $c$ -axis are calculated by the inverse iteration method. The wave function of an exact eigenstate locates selectively on a particular set of atoms and clusters and such a spatial pattern is very sensitive to an eigen energy. We believe that the observed cluster-specific distribution of wave functions relates strongly to the anomalous DOS with dense spikes.<sup>11</sup> The wave functions of the eigenstates near the Fermi energy  $E_F$  ( $\approx -0.04$  Ry) favorably spread over large atom clusters as seen in Fig. 1 and the wave functions at  $-0.5$  Ry spread over both large and small atom clusters. This fact shows that the small clusters play the role of glue and stabilize energetically the local cluster arrangement.

Eigenfunctions in the LMTO method are linear combinations of the muffin-tin orbitals  $\chi_{\mathbf{R}L}$  as  $\psi(\mathbf{r}) = \sum_{\mathbf{R}L} C_{\mathbf{R}L} \chi_{\mathbf{R}L}(\mathbf{r})$ , where  $\mathbf{R}$  and  $L$  denote atomic positions and the angular momentum components, respectively. The participation ratio of an eigenstate is defined as

$$P(\psi) = \frac{(\sum_{\mathbf{R}L} |C_{\mathbf{R}L}|^2)^2}{\sum_{\mathbf{R}L} |C_{\mathbf{R}L}|^4}, \quad (1)$$

which gives the measure of the spatial extent of wave functions; e.g.,  $P \approx 1$  for localized wave functions and  $P \approx N$  for extended wave functions ( $N$  is the total number of atoms).

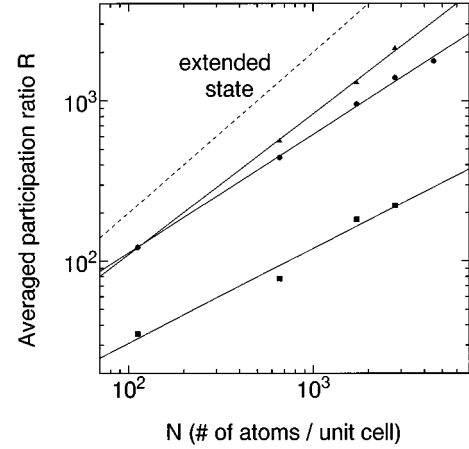


FIG. 2. The participation ratio averaged over about 50 eigenstates around the Fermi energy ( $\circ$ ), at  $-0.2$  Ry ( $\square$ ) and  $-0.5$  Ry ( $\triangle$ ) as a function of the number of atoms  $N$  in a unit cell. The dashed line shows  $P \propto N$  which is for uniformly extended states.

Figure 2 shows  $P(\psi)$  averaged over about 50 exact eigenstates around  $E_F$  as a function of  $N$ . The results clearly show that the participation ratio can be scaled by the power law. The value of the power-law index around  $E_F$  is nearly 0.74 ( $P \propto N^{0.74}$ ) and not universal. In fact, the value of the index depends on the range of eigenenergies, because the components of an eigenstate, angular momentum components, and atomic species depend sensitively on its eigenenergy. For example, the states at  $-0.2$  Ry are mainly of Co  $3d$  orbitals ( $P \propto N^{0.59}$ ) and at  $-0.5$  Ry of the transition metal  $4s$  and Al  $3s, 3p$  orbitals ( $P \propto N^{0.88}$ ). The power-law dependence of  $P$  does not necessarily imply that a wave function obeys a simple power law with a *single center* of amplitude. Actually, amplitudes of a wave function distribute on some specific groups of atoms like a percolated “stain”<sup>7</sup> as shown in Fig. 1 and they follow the power law on average. The transport properties may be very special because of this peculiar extension of a wave function of an eigenstate. Randomness smears out the particular pattern of an individual eigenstate. Furthermore, randomness makes the distribution of eigenenergies much smoother with uniform energy differences.

Zero-temperature dc conductivity is expressed by the Kubo formula as

$$\sigma_{\alpha\beta} = \frac{2\pi e^2 \hbar}{V} \int dE \left( -\frac{df}{dE} \right) \sum_i \delta(E - E_i) D_i^{\alpha\beta}(E), \quad (2)$$

$$D_i^{\alpha\beta}(E) = -\frac{1}{\pi} \lim_{\gamma \rightarrow 0^+} \text{Im} \left\langle i \left| \hat{v}_\alpha \frac{1}{E + i\gamma - \hat{H}} \hat{v}_\beta \right| i \right\rangle \\ \equiv \lim_{\gamma \rightarrow 0^+} D_i^{\alpha\beta}(E; \gamma), \quad (3)$$

where  $\alpha$  and  $\beta$  refer to the directions parallel to the quasiperiodic plane,  $\hat{H}$  is the TB-LMTO Hamiltonian, and  $\hat{v}_\alpha = 1/(i\hbar)[\hat{x}_\alpha, \hat{H}]$  is the velocity operator. The function  $f$  is the Fermi-Dirac distribution function and  $V$  is the volume of

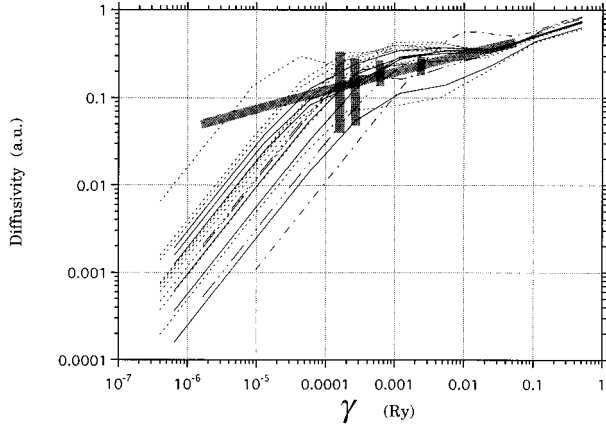


FIG. 3. Log-log plot of the diffusion constant as a function of  $\gamma$  for several eigenstates near the Fermi energy ( $-0.0425$  Ry  $< -0.0410$  Ry) in systems of several different sizes. Dotted line:  $N=110$ , three dots-dashed lines:  $N=644$ , solid lines:  $N=1686$ , dotted lines:  $N=2728$ . Vertical shaded bars indicate positions of crossover points and the width of the fluctuation (from left to right, in the order of the system size  $N$ ). The behavior  $D \sim \gamma_{\text{cr}}^{0.25 \dots}$  is also shown by a shaded strip.

the unit cell. This equation defines the diffusion constant  $D_i^{\alpha\beta}(E_i)$  of the  $i$ th eigenstate of an energy  $E_i$ . The conductivity in a finite crystalline system should grow in proportion to the system size and Eq. (2) actually does.

The  $\gamma$  in Eq. (3) should, in a strict sense, go to zero after the thermodynamic limit,  $V \rightarrow \infty$ , is taken. In the case of finite temperatures or randomness in the system, the  $\gamma$  should remain finite. We calculate  $D_i^{\alpha\alpha}(E; \gamma)$  with a varying parameter  $\gamma$  in several finite systems of volume  $V$ . When  $\gamma$  is unphysically small (much smaller than the averaged level interval  $\delta E$  proportional to  $1/N$ ), then we expect a behavior  $D_i^{\alpha\alpha}(E; \gamma) \sim \gamma$ .

The diffusion constant  $D_i^{\alpha\alpha}(E_i; \gamma)$  is shown in Fig. 3, as a function of  $\gamma$ , for various unit-cell sizes and for various eigenstates near the Fermi energy. Different behavior of the diffusion constant can be clearly observed in two separate  $\gamma$  regions: one is the behavior  $D \propto \gamma$  and the other is a slowly varying  $D$ . The crossover value  $\gamma_{\text{cr}}$  is the smallest limit of physically acceptable  $\gamma$  in a system of finite size. As the unit-cell size is enlarged, the crossover region gradually shifts to a smaller  $\gamma$  side and a smaller  $D$  value. The crossover point  $\gamma_{\text{cr}}$  and the distribution width of  $D$  at  $\gamma_{\text{cr}}$  is shown in Fig. 3 by a vertical shaded bar. The fluctuation width increases with increasing system size. The system size might still be too small but we could fit a curve  $D \sim \gamma_{\text{cr}}^{0.25 \dots}$  for this behavior of the crossover point as shown in Fig. 3 by another shaded strip. The power-law index is not universal and dependent on the energy region. The resultant value  $\gamma_{\text{cr}}$  of the crossover point seems slightly larger than the average level interval  $\delta E$ , which is equal to bandwidth ( $\sim 2$  Ry)/number of orbitals ( $9 \times N$ ) and is proportional to  $(1/N)$ . The diffusion constant  $D$  may be written as  $D \sim \langle r^2 \rangle \gamma_{\text{cr}}$ , where  $\langle r^2 \rangle$  is a spatial extent of a wave function and  $\hbar/\gamma_{\text{cr}}$  is the mean free time. Once assuming a wave function is not strongly localized, we obtain  $\langle r^2 \rangle \sim L^2$ , where  $L$  is the effective relaxation length proportional to the linear

dimension of the system  $\sqrt{N}$ . We assume a scaling relation  $\gamma_{\text{cr}} \sim L^{-2\beta}$  and the index  $\beta$  may be the scaling index of the density of states around the Fermi energy. By using the observed behavior  $D \sim \gamma_{\text{cr}}^{1-1/\beta} \approx \gamma_{\text{cr}}^{0.25 \dots}$ , one obtains an estimation  $\beta \sim 1.33 \dots$  and then the diffusion constant of the finite system can be written as  $D \sim L^{-2(\beta-1)} \sim N^{-0.33 \dots}$ . The resultant behavior  $\gamma_{\text{cr}} \approx \Delta E \sim N^{-1.33 \dots}$ , where  $\Delta E$  is the effective interval of eigenenergies, may be consistent with observed existence of a dense set of spikes in the density of states. Moreover, this conclusion indicates the enhancement of the dense spikes, both density and width, in larger systems. The Fermi energy  $E_F$  locates in the pseudogap where level intervals may be much larger than  $\delta E$ . Therefore, the observation  $\gamma_{\text{cr}} \sim \delta E$  may not be inconsistent with the result  $\gamma_{\text{cr}} \sim N^{-1.33 \dots}$ , because of the rather small system size in the present calculation.

The diffusion constant  $D$  in an infinite system may be small but decreasing rate with increasing  $N$  is very slow. Actually, even though we could prepare a system of a value  $\gamma_{\text{cr}}$  of  $10^{-6}$  Ry ( $\sim 1$  K), the diffusion constant would become smaller only by a factor of 10 in comparison with a system of  $\gamma \sim 10^{-2}$  Ry.

The resistivity may be calculated by using Eq. (2). If we adopt the simplest approximation for the DOS to be equal to the averaged value, we obtain a value of several thousands of  $\mu\Omega$  cm even for  $\gamma_{\text{cr}} \sim 10^{-5}$  Ry. Experimentally observed resistivity in decagonal Al-Cu-Co is  $340 \mu\Omega$  cm parallel to the quasiperiodic plane. Because the distribution of the eigenenergies is not smooth but consists of a set of sharp spikes,<sup>7,9-11</sup> the resulting resistivity in large systems should be fluctuating very rapidly and observed resistivity can be much larger than the above value. Furthermore, the observed resistivity should be very sensitive to atomic composition, sample preparation, and the material itself.

The temperature and randomness dependence of the observed resistivity can be discussed in relation to the scaling behavior of the diffusion constant. These two factors, temperature and randomness, cause incoherent electron scattering and then  $\gamma$  increases (for example,  $\gamma_0$ ) or the mean free path decreases. As a result, the whole system becomes equivalent to an array of perfect block quasicrystals of a length  $L_0 \sim \gamma_0^{-1/(2\beta)}$ . The bulk diffusion constant can be obtained by averaging over those of finite systems of the length  $L_0$ .

In conclusion, the present calculation shows the spatial extent of eigenstates and the power-law behavior of the diffusion constant in realistic quasicrystalline systems. The wave functions spread over the whole system, though the weight of the wave functions distributes over specific groups of atoms or clusters. In average, the spatial extent of the wave functions obeys the power law. The anomaly of the transport properties in quasicrystals is ascribed to both the scaling behavior of the wave functions and the diffusion constant, in addition to the low DOS value at  $E_F$ . We believe now that these properties are common to icosahedral and decagonal quasicrystals.

The numerical calculation was carried out in the computer facilities at the Institute of Molecular Science at Okazaki, Japan.

- <sup>1</sup>F. S. Pierce, S. J. Poon, and Q. Guo, *Science* **261**, 737 (1993); B. D. Biggs, S. J. Poon, and N. R. Munirathnam, *Phys. Rev. Lett.* **65**, 2700 (1990).
- <sup>2</sup>T. Klein, C. Berger, D. Mayou, and F. Cyrot-Lackmann, *Phys. Rev. Lett.* **66**, 2907 (1991).
- <sup>3</sup>K. Kimura, K. Kishi, T. Shibuya, T. Hashimoto, and S. Takeuchi, *Mater. Sci. Eng. A* **133**, 94 (1991); U. Mizutani, Y. Sakabe, T. Shibuya, K. Kishi, K. Kimura, and S. Takeuchi, *J. Phys. Condens. Matter* **2**, 6169 (1990).
- <sup>4</sup>C. C. Homes, T. Timusk, X. Wu, Z. Altounian, A. Sahnoune, and J. O. Ström-Olsen, *Phys. Rev. Lett.* **67**, 2694 (1991).
- <sup>5</sup>S.-y. Lin, X.-m. Wang, L. Lu, D.-l. Zhang, L. X. He, and K. X. Kuo, *Phys. Rev. B* **41**, 9625 (1990); S. Martin, A. F. Hebard, A. R. Kortan, and F. A. Thiel, *Phys. Rev. Lett.* **67**, 719 (1991).
- <sup>6</sup>D. N. Basov, T. Timusk, F. Barakat, J. Greedan, and B. Grushko, *Phys. Rev. Lett.* **72**, 1937 (1994).
- <sup>7</sup>T. Fujiwara, S. Yamamoto, and G. Trambly de Laissardière, *Phys. Rev. Lett.* **71**, 4166 (1993).
- <sup>8</sup>D. Mayou, C. Berger, F. Cyrot-Lackmann, T. Klein, and P. Lanco, *Phys. Rev. Lett.* **70**, 3915 (1993).
- <sup>9</sup>T. Fujiwara, *Phys. Rev. B* **40**, 942 (1989); T. Fujiwara and T. Yokokawa, *Phys. Rev. Lett.* **63**, 333 (1991).
- <sup>10</sup>G. Trambly de Laissardière and T. Fujiwara, *Phys. Rev. B* **50**, 5999 (1994).
- <sup>11</sup>G. Trambly de Laissardière and T. Fujiwara, *Phys. Rev. B* **50**, 9843 (1994).
- <sup>12</sup>E. Belin and A. Traverse, *J. Phys. Condens. Matter* **3**, 2157 (1991); M. Mori, S. Matuo, T. Ishimasa, T. Matuura, K. Kamiya, H. Inokuchi, and T. Matsukata, *ibid.* **3**, 767 (1991).
- <sup>13</sup>S. Yamamoto and T. Fujiwara, *Phys. Rev. B* **51**, 8841 (1995).
- <sup>14</sup>K. Kimura and S. Takeuchi, in *Quasicrystals: The States of the Art*, edited by D. P. DiVincenzo and P. J. Steinhardt (World Scientific, Singapore, 1991).
- <sup>15</sup>T. Fujiwara and H. Tsunetsugu, in *Quasicrystals: The States of the Art*, (Ref. 14); H. Tsunetsugu, T. Fujiwara, K. Ueda, and T. Tokihiro, *J. Phys. Soc. Jpn.* **55**, 1420 (1986).
- <sup>16</sup>F. Laçon and L. Billard, *J. Phys. France* **49**, 249 (1988).
- <sup>17</sup>S. E. Burkov, *Phys. Rev. Lett.* **67**, 614 (1991); *J. Phys. I France* **2**, 695 (1992).
- <sup>18</sup>K. Hiraga, W. Sun, and F. J. Lincoln, *Jpn. J. Appl. Phys.* **30**, L302 (1991).
- <sup>19</sup>O. K. Andersen and O. Jepsen, *Phys. Rev. Lett.* **53**, 2571 (1984).
- <sup>20</sup>R. Haydock, in *Solid State Physics*, edited by F. Seitz and D. Turnbull (Academic Press, New York, 1980), Vol. 35, p. 215; T. Fujiwara, *J. Non-Cryst. Solids* **61&62**, 1039 (1984).